**RESEARCH ARTICLE**

OPEN ACCESS  Check for updates

# Monitoring Forest Cover Change and Encroachment Risk Mapping Using the Normalized Difference Fraction Index (NDFI): A Case Study of Gunung Halimun Salak National Park, Indonesia

Ahmad Fahrur Rizqi[a], Adisti Permatasari Putri Hartoyo[a,b], Mursalina Nur Buana[a], Novia Damayanti[a], David Anderson Lubis[a], Yurico Bakhri[a]

[a] Department of Silviculture, Faculty of Forestry and Environment, IPB University, IPB Dramaga Campus, Bogor, 16680, Indonesia
[b] Center for Environmental Research, IPB University, IPB Dramaga Campus, Bogor, 16680, Indonesia

**ABSTRACT**

Gunung Halimun Salak National Park (GHSNP) is one of the most biodiversity-rich protected areas in Java, yet it remains highly vulnerable to deforestation and forest degradation. This study examines forest cover dynamics from 1994 to 2024 and projects village-level encroachment risk for 2034. Landsat 5 TM, Landsat 7 ETM+, and Landsat 8–9 OLI imagery were processed in Google Earth Engine to generate the Normalized Difference Fraction Index (NDFI) using spectral mixture analysis of GV, NPV, soil, and shade fractions. Changes in NDFI (ΔNDFI) were used to classify degradation, deforestation, regrowth, and intact forest. Encroachment risk mapping was modeled using a 3 × 3 kernel neighborhood with two analytical approaches: the sum of risk weight and the majority of risks around. Forest cover declined by 19,424 ha between 1994 and 2004, largely driven by illegal encroachment linked to governance uncertainty in 2003. An increase of 6,678 ha during 2004–2014 reflects the impact of restoration initiatives and strengthened area protection, although a subsequent decline of 1,992 ha occurred between 2014 and 2024 due to renewed encroachment. Model evaluation indicates low predictive performance for both kernel methods (Precision 4%). Despite this limitation, areas of elevated risk consistently appeared along forest edges near settlements and footpath access routes. Citorek Kidul was identified as the village most susceptible to encroachment in 2034. Improving the accuracy of encroachment prediction will require the integration of socio-economic drivers and advanced machine-learning approaches capable of capturing the complex and non-linear patterns of forest encroachment.

## Introduction

Gunung Halimun Salak National Park (GHSNP) is one of the remaining important protected areas for biodiversity, but it is now under threat. The GHSNP is the largest tropical rainforest area on the island of Java and is home to hundreds of animal species, including 32 endemic Java bird species and a key population of the critically endangered Javan hawk-eagle (*Nisaetus bartelsi*) [1,2]. The GHSNP continues to face pressure from human activities that have been proven to cause forest cover loss, despite its status as a protected area [3]. These pressures stem from the socio-economic needs of the community and land-use conflicts rooted in a long history that continues to threaten the integrity of the area [4,5]. Despite ongoing restoration initiatives, the persistent threat of forest encroachment underscores the need for more robust and proactive protection strategies. The conservation issues in the GHSNP reflect a broader crisis experienced by mountain rainforests worldwide. Mountain ecosystems are centers of global biodiversity with unique environmental conditions that give rise to a wealth of unique and specialized species [6,7].

However, this also makes mountain ecosystems highly vulnerable to habitat loss. Forest clearing and degradation are the greatest threats that could trigger the extinction of endemic species on densely populated islands, such as Java [8]. Therefore, the successful discovery of effective protection methods for GHSNP will have a broad impact. The conservation challenges observed in GHSNP mirror a wider crisis affecting mountain rainforests across the world. Mountain ecosystems serve as global biodiversity strongholds, shaped by distinctive environmental conditions that support highly specialized and often narrowly distributed species [6,7]. Yet these same ecological features render them exceptionally vulnerable to habitat loss. On densely populated islands such as Java, forest clearing and degradation pose serious risks and may accelerate the extinction of endemic taxa [8]. Consequently, identifying effective protection strategies for GHSNP is not only critical for the park itself but also holds broader significance for the conservation of mountain forest ecosystems in similar socio-ecological settings.

Efforts to mitigate these threats are often constrained by the limitations of current monitoring practices. Most monitoring programs still rely heavily on satellite-based indices such as the Normalized Difference Vegetation Index (NDVI), which is effective for detecting broad-scale forest loss but less responsive to subtle disturbances, including low-intensity logging and canopy thinning [9]. Moreover, these approaches are predominantly retrospective, documenting damage only after it has occurred rather than supporting early intervention. Such reactive strategies are particularly inefficient for managers operating under limited resources. These constraints highlight the need for a more proactive framework capable of anticipating areas that are likely to experience future encroachment, thereby enabling targeted preventive measures.

Responding to this gap, the present study applies an integrated framework to monitor long-term forest change and predict encroachment risk in GHSNP. Using the Google Earth Engine (GEE) platform, we assessed forest dynamics over a 30-year period (1994–2024) through the Normalized Difference Fraction Index (NDFI), which offers improved sensitivity to both degradation and deforestation by distinguishing healthy vegetation, senescent vegetation, and exposed soil [10]. The key contribution of this study lies in combining detailed historical diagnostics with a spatially explicit predictive risk model. Based on the REDD+ risk mapping approach (JNR) (VT0007 Verra), a forest encroachment vulnerability forecast map was compiled for the next ten years (2024–2034). The Jurisdictional and Nested REDD+ (JNR) Framework developed by Verra offers a systematic approach to evaluating the risks of deforestation and degradation by examining recurring patterns of forest change within a landscape. In this study, the JNR concept is used to guide the identification of areas within GHSNP that show repeated signs of forest disturbance, highlighting zones that may be more vulnerable to future forest encroachment. In addition, this study provides recommendations for village locations vulnerable to forest encroachment in the GHSNP.

## Materials and Methods

### Research Location and Time

This study was conducted in the GHSNP area, located at the western end of the West Java Province, Indonesia. Its precise coordinates are between 6°30'–6°50' North latitude and 106°25'–106°55' East longitude, with an area of 113,357 ha. There are 115 villages within the national park area, spread across three different regencies: Bogor Regency and Sukabumi Regency in West Java Province and Lebak Regency in the Banten Province. The period used in the research for monitoring forest changes ranged from 1994 to 2024, while the forest encroachment risk map was taken from 2014 to 2024 for model testing and 2024 to 2034 for future projections. The intact forest condition in 1994 was used as a baseline for the primary forest boundary to clarify deforestation and degradation in the NDFI change map. A schematic representation of the study is shown in Figure 1.

### Tools and Materials

The tools used in this study included the GEE and ArcGIS Pro 3.4. The materials used in this study included the administrative boundaries of villages and districts from the geospatial information agency, administrative boundaries of GHSNP from the Ministry of Forestry, Landsat 5 Thematic Mapper image (data collection in 1994), Landsat 7 Enhanced Thematic Mapper Plus (data in 2004), and Landsat 8 and 9 Operational Land Imagery (data in 2014 and 2024).

### Research Procedure

The research procedure was divided into four stages: the process began with the collection of initial image data. This was followed by the second stage, which involved the generation and classification of the NDFI.

The third stage consisted of forest encroachment risk map generation. The final stage focused on the validation process to assess the accuracy of the generated map. The complete research process is shown in Figure 2, and the details are explained in each procedural subsection.
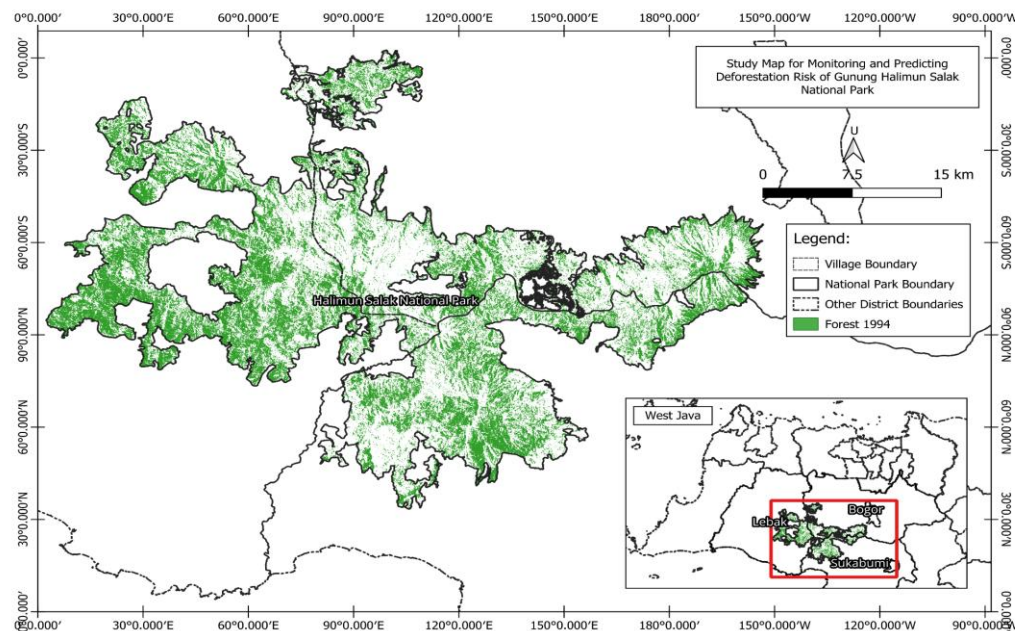


**Figure 1.** Study area of monitoring forest cover change and risk map of forest encroachment in GHSNP. The green-shaded area represents the 1994 forest cover used as the baseline observation boundary for all NDFI and ΔNDFI analyses. Forest changes outside this extent were excluded because national forest-status definitions classify primary and secondary forests based on early-1990s historical cover. This baseline ensures consistent temporal comparison and delineates the spatial domain for all subsequent forest-change and risk assessments.
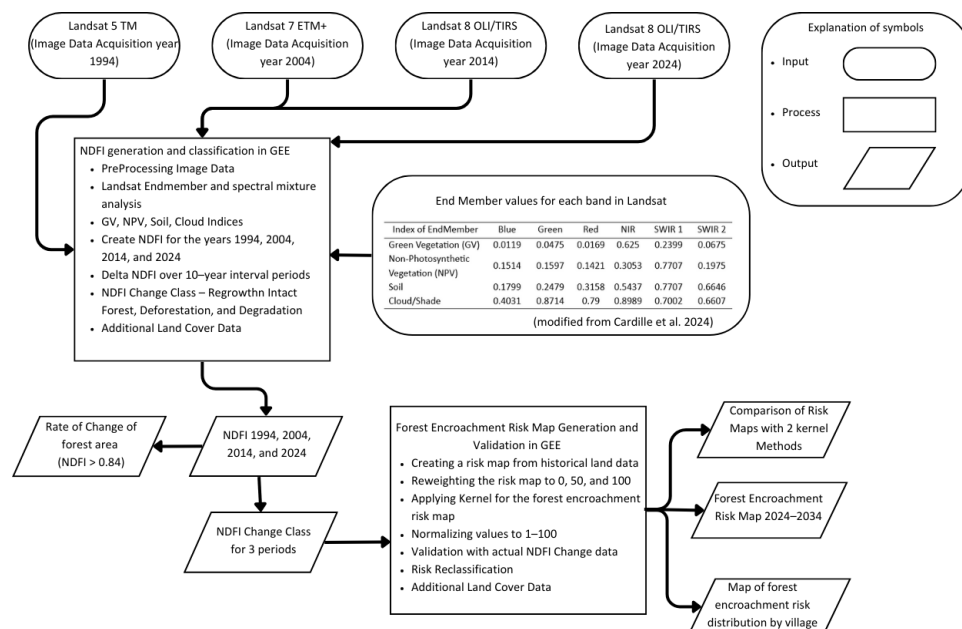


**Figure 2.** Workflow of the multi-temporal analysis for forest change detection and encroachment risk prediction in GHSNP. The flowchart illustrates the main stages of the study, beginning with Landsat data preprocessing and the generation of NDFI. It is followed by ΔNDFI classification to identify changes in forest condition across the study period. The workflow also shows the kernel-based modeling applied to predict future forest–encroachment risk and the validation steps used to assess model performance. This framework integrates all multi-temporal analyses conducted on the GEE platform.

## Image Data Collection

The initial stage of the research began with the collection of Landsat satellite image data from various sensors (Landsat 5, 7, 8, and 9) at four time points: 1994, 2004, 2014, and 2024. Each data collection from GEE was selected in the form of Surface Reflectance (SR) and filtered based on a one-year period (January to December) with less than 60% cloud coverage. The image dataset was then cloud-masked with the QA_PIXEL band, calibrated, and combined into a single image using the median method. The preprocessing steps ensured that the resulting dataset remained consistent and reliable, thereby establishing a robust foundation for the subsequent NDFI derivation and classification processes.

## NDFI Derivation and Classification

At this stage, the analysis focused on assessing forest conditions and detecting changes through the use of the NDFI. NDFI was computed using a spectral mixture analysis (SMA) approach, which decomposed the spectral signal into four primary components: green vegetation (GV), non-photosynthetic vegetation (NPV), soil, and cloud/shade, derived from the endmembers reported in [10,11]. The classification procedure ensured that forest condition categories were consistently defined and comparable across the examined years. The resulting outputs were subsequently used as inputs for analyzing temporal dynamics and predicting potential encroachment areas. NDFI was calculated using equations 1 and 2.

$$GV_{shade} = \frac{GV}{100 - shade} \tag{1}$$

$$NDFI = \frac{GV_{shade} - (NPV + Soil)}{GV_{shade} + NPV + Soil} \tag{2}$$

The difference in NDFI between time periods (ΔNDFI) was utilized to detect and classify forest change. The analysis covered three observation periods, namely 1994–2004, 2004–2014, and 2014–2024. These changes were categorized into four classes based on ΔNDFI threshold values: 0.17 to 2 for regrowth forest, −0.16 to 0.16 for intact forest, −0.42 to −0.17 for degradation, and −2 to −0.43 for deforestation. To maintain consistency in the spatial analysis, changes were calculated only for areas that were classified as intact forest in 1994 (NDFI > 0.84). To analyze the influence of other land covers, the ΔNDFI map for 2014–2024 was combined with the Dynamic World V1 land cover classification, sourced from the World Resources Institute (WRI), to fill in areas with null values. The map was reclassified into 12 classes: regrowth forest, intact forest, degradation, deforestation, water, trees, grass, inundation, agriculture, shrubs, built-up areas, and open land.

## Forest Encroachment Risk Map Generation and Validation

A forest encroachment risk map was created by combining and weighting the classifications from the previous two periods. As a reference for the 2014–2024 forest encroachment risk map, we used a combination of the 1994–2014 intact forest map, which was given a weight of 1, deforestation and degradation 1994–2004 was given a weight of 2, and deforestation or degradation 2004–2014 was given a weight of 3. These scores were then transformed into explicit weighting values of 0, 50, and 100 to create quantitative scores proportional to the categorization: no risk, medium risk, and high risk. These scores were spatially recalculated using a 3 × 3 kernel window with two different methods: reduced neighbourhood (majority of risks around) and convolve (sum of risk weight) to compare and determine the most accurate method.

Risk maps were normalized to a scale of 1 to 100 based on the 1st and 99th percentiles, respectively. Next, these predictions were validated against the actual conditions of 2014–2024 based on the pre-processed NDFI Change from 2014 to 2024. Each map was reclassified into not at risk and at risk, where in the forest encroachment risk map, values below 50% were categorized as not at risk and values above 50% were categorized as at risk, whereas in the NDFI Change map, intact forest was categorized as not at risk of degradation and deforestation was categorized as at risk. The classification results of the two maps were the basis for validation tests in the evaluation matrix, in the form of overall accuracy (OA), precision, recall, F1-score, intersection over union (IoU), and kappa coefficient (KC) [12] as shown in the following equation:

$$AO = \frac{TP + TN}{TP + TN + FP + FN} \tag{3}$$

$$KC = \frac{N\sum(TP + TN) - \sum(TN + FN)}{N^2 - \sum(TN + FN)} \tag{4}$$

$$precision = \frac{TP}{TP + FP} \tag{5}$$

$$recall = \frac{TP}{TP + FN} \tag{6}$$

$$F - Measure = \frac{2 \times precision \times recall}{precision \times recall} \qquad (7)$$

$$IoU = \frac{TP}{TP + FP + FN} \qquad (8)$$

where TP, TN, FN, and FP represent the number of pixels of the true forest change. True positives (TP) refer to areas predicted to be at risk of forest encroachment that experience encroachment. Conversely, true negatives (TN) are areas predicted not to be at risk that do not experience encroachment. A false positive (FP) occurs when the model predicts an area as prone to forest encroachment, but no encroachment takes place in that location. Meanwhile, false negatives (FN) describe a condition in which areas that experience encroachment are not detected by the model as being at risk.

The same approach was used for the 2024–2034 forest encroachment risk map with the intact forest, deforestation, and degradation data collection periods from the previous two periods 2004–2014 and 2014–2024. The forest encroachment risk map was then classified into five risk classes: very low (< 9.9%), low (10.0–20.9%), medium (21.0–33.8%), high (33.9–48.2%), and very high (48.3–100%) [13]. The area of each risk class was quantified in hectares (ha). This quantification was intended to showed a clear comparison across different risk levels.

### Data Analysis

The analysis process started with compiling the result of the NDFI classification to generate forest area values for each observation years. These values was used as a foundation for evaluating forest cover dynamics and interpreting the direction of change across three time periods. The temporal comparison enabled the identification of both forest loss and regrowth patterns, which were essential for understanding long-term ecological processes. To maintain analytical consistency, only areas categorized as intact forest in the baseline year were included in the calculations, minimizing potential bias from other land cover types. Forest area data obtained from NDFI at four observation times (1994, 2004, 2014, and 2024) was then examined to estimate the rate of forest area changes using the formula provided by Puyravaud [14] as follow:

$$r = \left(\frac{1}{t2 - t1)}\right) \times ln\, ln\, (\frac{A2}{A1}) \qquad (9)$$

where r = rate of change, t1 = initial observation time, t2 = final observation time, A1 = Initial year forest area, and A2 = final year forest area.

## Results and DIscussion

### Results

The NDFI map (Figure 3) that forest cover in the GHSNP changed with fluctuating patterns duringthe observation periods of 1994, 2004, 2014, and 2024. Visually, there appears to be a decrease in forest cover from 1994 to 2004, followed by an increase during the 2004 to 2014 period, but then a decline is seen again in 2024, although it is not as severe as in previous periods. This is evidenced by the intact forest data from 1994 to 2024, which shows a sharp decrease of 19,424.27 ha, followed by an increase of 6,678.13 ha in the following period, and then another decrease, although not very significant, of approximately 1,992.1 ha. The forest change rate data over the three observation periods showed a similar pattern, where only the period from 2004 to 2014 experienced an increase in forest cover of 0.034% annually. The period 1994–2004 showed a decrease in forest cover change with the highest rate of –0.079 % per year. The decline in land cover also occurred again in the 2014–2024 period at a smaller rate, approximately –0.009% per year.

The distribution of changes in NDFI values over the three observation periods in the GHSNP (1994–2004, 2004–2014, and 2014–2024) is visualized in the form of a histogram in Figure 4. The visualization results indicated that the ΔNDFI values across the three observation periods exhibited a symmetrical distribution. However, closer inspection of the distance between the of each peak and the value of 0. Based on the NDFI change threshold, positive values (NDFI > 0.17) represent areas undergoing regrowth, whereas negative values (NDFI < –0.17) imply forest damage (degradation and deforestation). If the values are approximately 0, it indicates no significant changes in the forest cover condition (intact forest). Throughout the three periods, a general trend can be observed in1994–2004, forest damage was more dominant, causing the distribution peak to trend towards the negative side of 0.
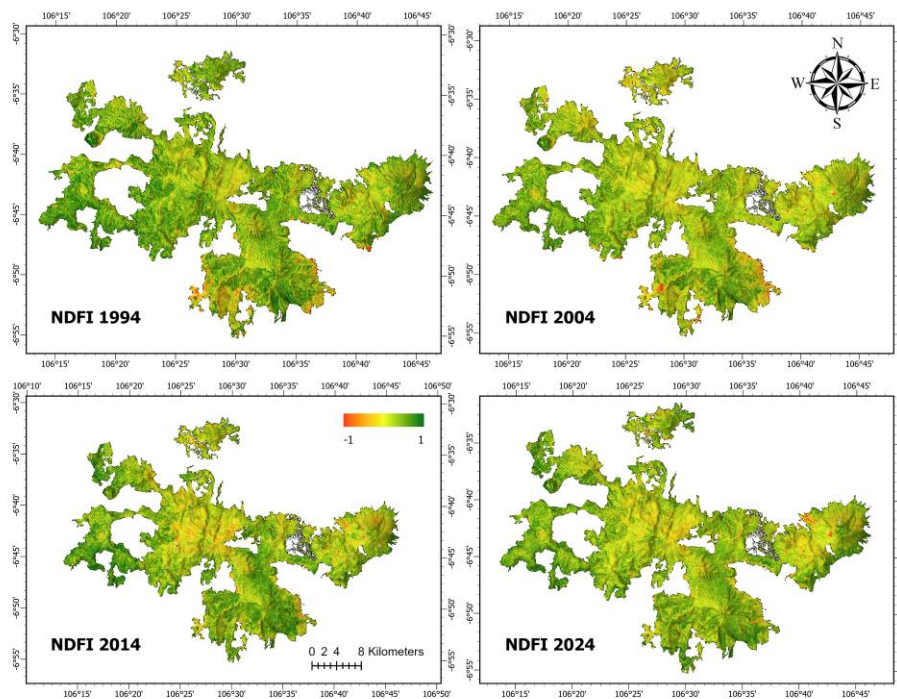
**Figure 3.** NDFI Map of GHSNP for the years 1994–2024. The maps show NDFI values ranging from –1 to +1, with green tones indicating dense and healthy forest, yellow-orange tones representing partially disturbed canopy, and red tones reflecting degraded or open areas. A consistent color gradient is applied across all years to allow direct comparison of forest canopy condition over time.
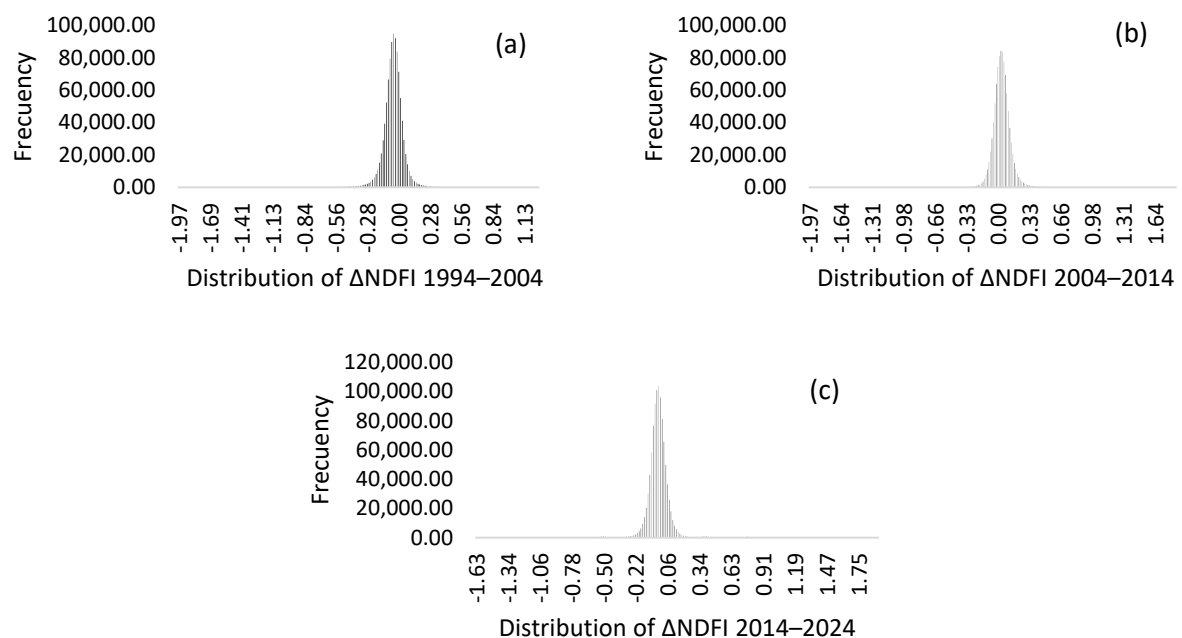


**Figure 4.** Distribution of NDFI change values in GHSNP during 3 observation periods: 1994–2004, 2004–2014, 2014–2024. The histograms illustrate the frequency of pixels across ΔNDFI values for each observation period. During 1994–2004, negative values predominated, reflecting high levels of forest degradation and deforestation. In 2004–2014, the distribution shifted toward positive values, indicative of forest regrowth. By 2014–2024, values are concentrated near zero, with moderate negative deviations, suggesting reduced but ongoing forest degradation. These results highlight the distinct dynamics of forest change across the three decades.

In contrast, during 2004–2014, regrowth was more dominant, shifting the distribution peak towards the positive side of 0. In the 2014–2024 period, the peak of the distribution moved closer to 0, indicating that more forest was maintained. This is evidenced by the data on areas of regrowth, degradation, and deforestation over the three periods in the GHSNP (Figure 5), where the highest degradation and deforestation occurred in the 1994–2004 period with a total of 3,103.25 ha, while the highest forest regrowth occurred in the 2004–2014 period. In the 2014–2024 period, the amount of degradation was almost balanced with regrowth, with a slight difference of 91.89 ha. The changes in degradation, deforestation, and regrowth are shown in Figure 6.
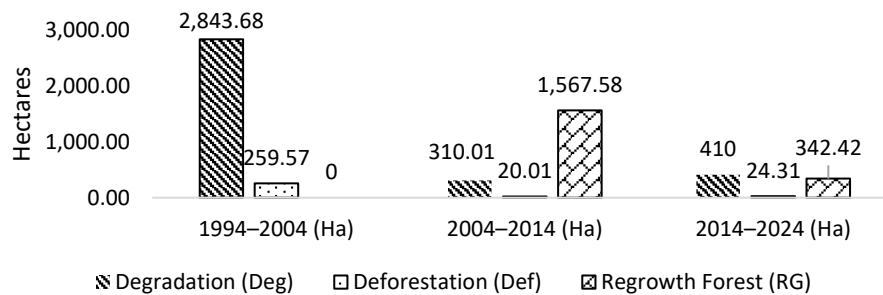


**Figure 5.** Changes in the extent of regrowth, deforestation, and forest degradation during the 3 observation periods in GHSNP. The figure summarizes the total area of each ΔNDFI class, showing severe degradation and deforestation in 1994–2004, followed by substantial regrowth in 2004–2014. The 2014–2024 period exhibits nearly balanced regrowth and degradation, indicating persistent but reduced forest disturbance.
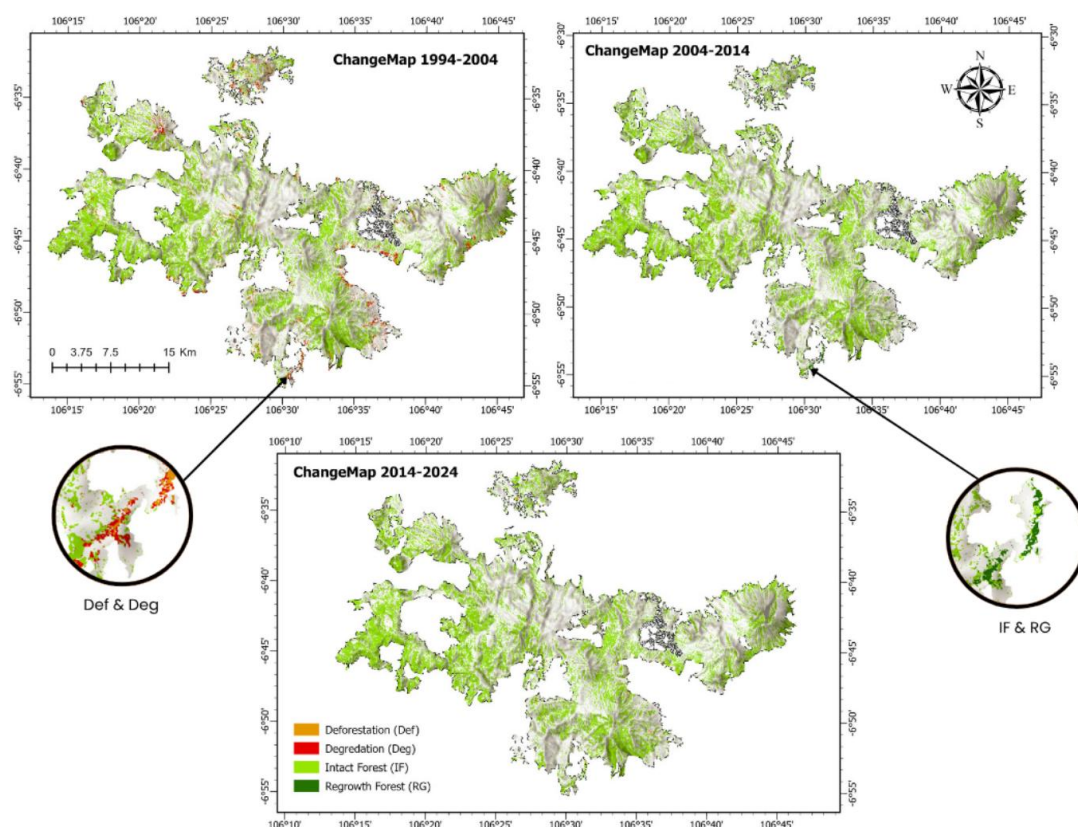


**Figure 6.** NDFI Change Class Map in GHSNP during 3 observation periods: 1994–2004, 2004–2014, 2014–2024. Areas in green represent intact forest, dark green indicates regrowth, orange denotes degradation, and red shows deforestation. The 1994–2004 map is dominated by red and orange patches around forest margins, while the 2004–2014 map shows expanded dark-green regrowth zones. In 2014–2024, red and orange areas became more scattered and localized, reflecting reduced but persistent disturbance.

Risk maps of forest encroachment in the GHSNP for the 2014–2024 period were created using two different kernel methods: "Sum of Risk Weight" and "Majority of Risks Around" (Figure 7). Both maps were compared to the actual conditions of the NDFI change map from 2014 to 2024, and their accuracy was tested, with the results shown in Figure 7. Both risk maps showed high OA values of approximately 93%; however, when examined more closely using other evaluation metrics such as precision, recall, F1-score, and IoU, these values were relatively lower. The very low Kappa coefficient values (5–6%) indicate that the level of agreement between the prediction results and the reference is barely better than random guessing. The precision values of both models at only 4% suggest that most areas predicted to be at risk were not encroachment areas, reflecting a high number of false positives. The recall values for areas at risk of forest encroachment ranged from 22 to 24%, indicating that approximately 76 to 78% of areas that experienced encroachment were not detected by the prediction models. The F1-score of 7% and IoU of only 3–4% further reinforce the conclusion that the classification system has a very poor performance in detecting forest encroachment areas.
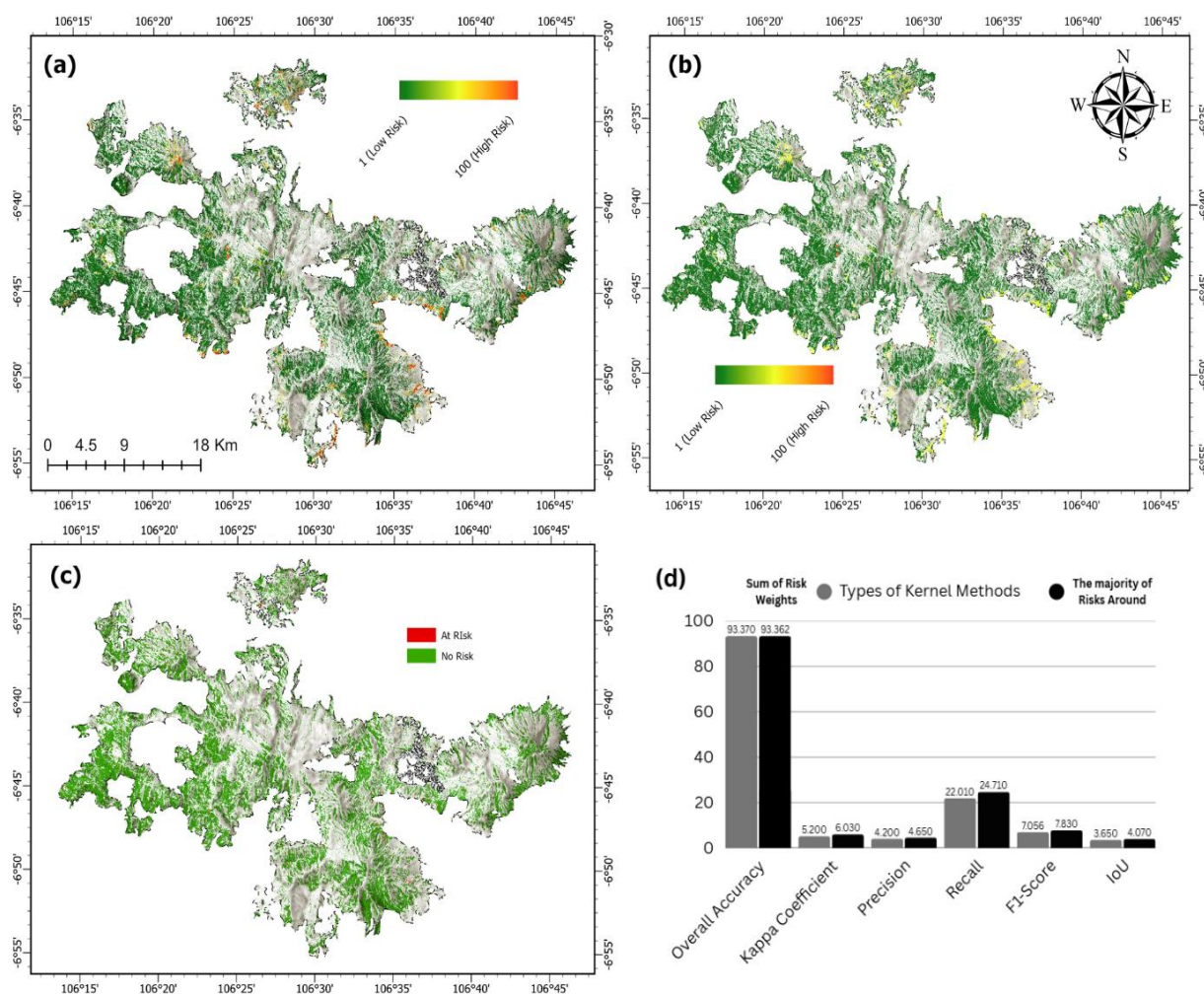


**Figure 7.** Comparison of forest encroachment risk maps 2014–2024 using two kernel methods: (a) sum of risk weight and (b) majority of risks around, with (c) actual NDFI Change Map Conditions 2014–2024, with (d) comparison of kernel methods accuracy parameters. Figures 7a and 7b highlight high-risk areas identified by the two kernel methods; however, these predicted patterns differ significantly from the actual forest encroachment observed from 2014–2024. Many locations classified as high-risk did not experience forest encroachment, while some areas with documented forest encroachment were not detected by the model. This discrepancy is further reflected in their very low precision data (4%), emphasizing the limitations of the reliability of kernel-based approaches in predicting forest expansion when relying solely on historical spatial patterns.

Further analysis was conducted on the forest encroachment risk data for the 2024–2034 period. This analysis was conducted within the administrative boundaries of the 115 villages located in the GHSNP (Figure 8 and Table 1). The results revealed that Citorek Kidul Village had the highest risk, with a predicted encroachment area of 149.36 ha. Meanwhile, Kiarasari Village had the lowest risk, with only 1.45 ha predicted to be encroached.
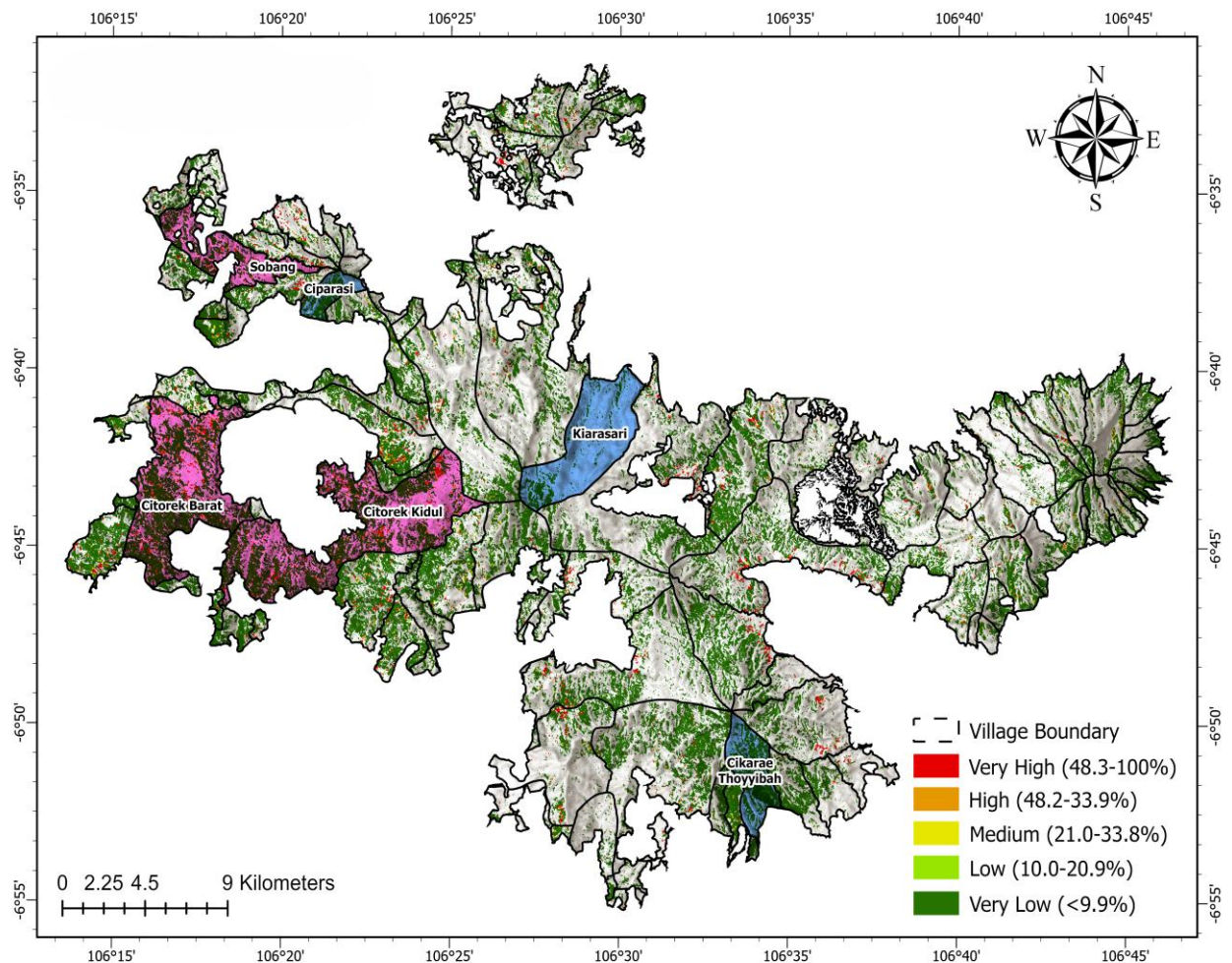


**Figure 8.** Predicted forest encroachment risk map for 2024–2034 in the GHSNP. The map presents five encroachment-risk classes as shown in the legend, ranging from very low to very high. Areas displayed in pink represent villages with the largest extent of predicted encroachment risk, while blue areas indicate villages with only a small at-risk extent. This color distribution highlights clear differences in predicted vulnerability across villages within GHSNP.

**Table 1.** The map presents five encroachment-risk classes as shown in the legend, ranging from very low to very high. Areas displayed in pink represent villages with the largest extent of predicted encroachment risk, while blue areas indicate villages with only a small at-risk extent. This color distribution highlights clear differences in predicted vulnerability across villages within GHSNP.

| Risk level | Village | Forest encroachment risk class in hectares | | |
|---|---|---|---|---|
| | | Very low | Medium | Very high |
| Highest | Citorek Kidul | 2,528.21 | 71.64 | 149.36 |
| | Citorek Barat | 2,188.41 | 57.19 | 128.34 |
| | Sobang | 549.68 | 4.57 | 46.99 |
| Lowest | Cipasari | 244.84 | 1.62 | 5.07 |
| | Cikare | 670.66 | 3.76 | 1.5 |
| | Kiarasari | 355.1 | 2.44 | 1.45 |

**Discussion**

The findings of this study revealed that forest cover in GHSNP has experienced fluctuating changes over the past three decades, reflecting the relationship between anthropogenic pressures and the effectiveness of policy interventions. The most severe period of degradation occurred between 1989 and 2004, when approximately 23,000 ha of forest were lost [15], likely due to several interrelated factors, including exploitative activities such as illegal logging, gold mining, and forest encroachment are the main drivers of biophysical damage. These factors were further intensified by legal uncertainty regarding the area's management status, especially in 2003 [16,17], which created a governance gap and accelerated deforestation. Moreover, population growth has increased demographic pressure [3], leading to the conversion of forest land into cropland and settlements to support the needs of local communities.

The forest recovery trend observed from 2004 to 2014 marked a major turning point, driven by shifts in policy and governance. The most important milestone was the reclassification of the area from production forest to a conservation national park through Minister of Forestry Decree No. 175/Kpts-II/2003. This regulation clarified the legal status of the landscape by consolidating former production and limited-production forest areas into a single conservation unit, thereby restricting extractive activities such as logging and mining and strengthening the authority of park managers in enforcing protection measures. This policy shift effectively halted large-scale logging and strengthened the legal framework for more intensive conservation efforts [18]. The success of this period was inseparable from the implementation of a participatory conservation approach initiated by the GHSNP Office [19] and strengthened by international cooperation with JICA.

Furthermore, a strong legal framework through a government regulation in 2011 enabled the launch of large-scale ecosystem restoration programs. The success of restoration initiatives, such as the "Halimun Salak Corridor" project supported by collaboration between star energy geothermal salak (SEGS) and the Kehati Foundation, as well as the involvement of various private companies (e.g., PT Antam and PT Aqua), shows that multi-stakeholder collaboration models are effective in mobilizing resources for land rehabilitation. The active involvement of local communities in these programs is a key factor in ensuring the sustainability and success of restoration in the field, as emphasized by previous studies [20,21].

Although the rate of deforestation has slowed, the return of the downward trend in forest area during the 2014–2024 period indicates that fundamental pressures on the GHSNP ecosystem remain persistent. This shows that policy interventions and restoration alone are insufficient if the root causes of economic problems and community conservation awareness have not been fully resolved [22]. Given the vast area of the GHSNP, monitoring that relies solely on officers is inefficient and ineffective. Therefore, adaptive management strategies that empower communities are essential. Agroforestry practices, which have been widely implemented in the buffer and traditional zones of the GHSNP [23,24], have emerged as strategic solutions. This model not only has the potential to mitigate tenure conflicts but also aligns community economic incentives with conservation goals, as they have a direct interest in preserving the area that is their source of livelihood.

The results of the forest encroachment risk map using the kernel method in this study showed a weak predictive model, as shown by the Precision and Kappa values. This was due to two factors: the influence of other variables on forest encroachment and the limitations of the kernel method. Forest encroachment is determined not only by patterns of historical occurrences but also by many other environmental and socio-economic variables, such as distance from agricultural land, distance from highways, elevation, distance from non-forest land, distance from mining areas, distance from settlements, and slope [25]. The distance from agricultural land and roads is the predictor variables that contribute most to the deforestation prediction model in the Peruvian Amazon Basin, each contributing almost 80% of the information required for prediction [13]. Beyond biophysical variables, socio-economic aspects such as population density, livelihood dependence on forest resources, and land tenure conflicts also play a decisive role in shaping encroachment patterns and should therefore be integrated into future risk modeling efforts. To address these issues, the Ministry of Environment and Forestry has promoted social forestry as a policy priority, which emerged from past debates over land tenure and community rights. Multiple stakeholders now support social forestry as an attractive win-win solution, noting that it can recognize communal rights, improve rural livelihoods, support conservation, and ultimately help resolve Indonesia's complex land conflicts [26].

Kernel methods are less efficient in handling high-dimensional data and capturing complex nonlinear patterns in deforestation data. More sophisticated approaches are needed for more reliable predictive analysis in the future. Thus, while this study provides a useful preliminary framework, it also highlights the need for future research integrating advanced deep learning methods. U-Net and ResNet have been shown to successfully

improve the accuracy of deforestation detection through multi-scale feature learning [27]. The integration of advanced satellite data (e.g., SAR) with convolutional neural network (CNN) architecture also shows great potential for mapping deforestation risk in complex tropical ecosystems [28–30]. Therefore, further research should focus on developing machine learning-based predictive models that integrate diverse datasets to produce more accurate decision-making tools for GHSNP managers and other authorized governance.

## Conclusions

Forest cover in Gunung Halimun Salak National Park has shifted significantly over the past three decades, with the largest loss recorded in 1994–2004 (19,424.27 ha), followed by regrowth in 2004–2014 (6,678.13 ha) and a moderate decline in 2014–2024 (1,992.1 ha). Citorek Kidul emerged as the area with the highest predicted encroachment risk for 2024–2034 (149.36 ha). These findings highlight the importance of conservation efforts by multiple stakeholders in protecting the forest ecosystem of GHSNP. Restoration efforts also should be prioritised in areas with the highest predicted risk of encroachment, supported by regular patrols to ensure that these locations remain well protected from future disturbances. Community involvement through social forestry plays a crucial role in achieving effective forest conservation as an important pathway for linking livelihood improvement with ecological protection. Further studies is needed to strengthen the predictive framework by incorporating socio-economic and accessibility factors, conducting field validation, and applying advanced approaches such as U-Net, ResNet, and SAR-based analyses to enhance the accuracy of encroachment risk forecasts and their relevance for conservation decisions.

## Authors Contributions

**AFR:** Conceptualization, Software, Methodology, Writing - Review & Editing; **APPH:** Conceptualization, Review, Investigation; **MNB:** Methodology, Writing - Review & Editing; **ND:** Methodology, Writing - Review & Editing; **DAL:** Methodology, Data Curation; **YB:** Writing - Review & Editing.

## AI Writing Statement

During the preparation of this work the authors used Paperpal in order to improve grammar and writing structure. After using this tool/service, the authors reviewed and edited the content as needed and take full responsibility for the content of the publication.

## Conflict of Interest

There are no conflicts to declare.

## References

1.  Prawiradilaga, D.M. Birds of Halimun Salak National Park, West Java, Indonesia: endemism, conservation and threatened status. *Treubia* **2016**, *43*, 47–70.

2.  Bramantio, M.D.; Prasetyo, L.B.; Mulyani, Y.A.; Pairah, P.; Septiana, W.; Erlan, M. Mapping priority areas for the restoration of Javan Hawk-Eagle habitat in Mount Halimun Salak National Park. *Sixth International Symposium on LAPAN-IPB Satellite* **2019**, *11372*, 422–431, doi:10.1117/12.2540818.

3.  Kurniawan, I.; Barus, B.; Pravitasari, A.E. Spatial modelling of land use change in Gunung Halimun Salak National Park and Its Buffer Area. *Journal of Regional and Rural Development Planning* **2017**, *1*, 270–286, doi:10.29244/jp2wd.2017.1.3.270-286.

4.  Hakim, N.; Murtilaksono, K.; Rusdiana, O. Land use conflict in Gunung Halimun Salak National Park, Lebak Regency. *Jurnal Sosiologi Pedesaan* **2016**, *4*, 128–138, doi:10.22500/sodality.v4i2.13377.

5.  Rochaedi, D.E.; Priatna, D.; Rahayu, S.Y.S. Ecosystem restoration conservation partnership as a conflict solution in Gunung Halimun Salak National Park. *Jurnal Penelitian Sosial dan Ekonomi Kehutanan* **2021**, *18*, 171–184.

6.  Wanie, C.M.; Nganjo, R.N. Tropical montane rain forest biodiversity and environmental sustainability in Cameroon's North Western Highlands. *International Journal of Forestry and Horticulture* **2018**, *4*, 1–11, doi:10.20431/2454-9487.0404001.

7.  Bañares-de-Dios, G.; Macía, M.J.; Arellano, G.; Granzow-de la Cerda, Í.; Vega-Álvarez, J.; Arnelas, I. Woody plant diversity along elevational gradients in Andean tropical montane forests. *Plant Diversity* **2024**, *46*, 491–501, doi:10.1016/j.pld.2024.03.005.

8.  Widodo, W.; Sulistyadi, E.; Istiadi, Y. Threat status of 56 bird species receiving little attention in Java. *Evolutionary Studies in Imaginative Culture* **2024**, *8*, 956–968, doi:10.70082/esiculture.vi.1165.

9.  Delgado-Moreno, D.; Gao, Y. Forest degradation estimation through trend analysis of annual time-series NDVI, NDMI and NDFI (2010–2020) using Landsat images. *Lecture Notes in Geoinformation and Cartography* **2022**, *vol*, 1–13, doi:10.1007/978-3-030-98096-2_11.

10. Souza Jr., C.M.; Roberts, D.A.; Cochrane, M.A. Combining spectral and spatial information to map canopy damage from selective logging and forest fires. *Remote Sensing of Environment* **2005**, *98*, 329–343.

11. Cardille, J.A.; Crowley, M.A.; Saah, D.; Clinton, N.E. *Cloud-based remote sensing with Google Earth Engine: Fundamentals and applications*; Springer Nature: New York, USA, 2024;

12. Guo, Y.; Long, T.; Jiao, W.; Zhang, X.; He, G.; Wang, W.; Zhang, X. Siamese detail difference and self-inverse network for forest cover change extraction based on Landsat 8 OLI satellite images. *Remote Sensing* **2022**, *14*, 1–20, doi:10.3390/rs14030627.

13. Rojas, E.; Zutta, B.R.; Velazco, Y.K.; Montoya-Zumaeta, J.G.; Salvà-Catarineu, M. Deforestation risk in the Peruvian Amazon Basin. *Environmental Conservation* **2021**, *48*, 310–319, doi:10.1017/S0376892921000291.

14. Puyravaud, J.P. Standardizing the calculation of the annual rate of deforestation. *Forest Ecology and Management* **2003**, *177*, 593–596.

15. Dewi, C.M. The economic conditions of the Kasepuhan Sinar Resmi community due to the expansion of the Gunung Halimun Salak National Park (TNGHS). *Jurnal Mozaik* **2018**, *10*, 22–25.

16. Zulkarnaen, R.N.; Iryadi, R.; Yudaputra, A. The effectiveness of landscape management of Gunung Halimun–Salak National Park. *Prosiding Seminar Nasional Masyarakat Biodiversitas Indonesia* **2020**, *6*, 501–506, doi:10.13057/psnmbi/m060104.

17. Ekrep, L.; Soetarto, E. The impact of national park's establishment towards agrarian structure and land management rights. *Jurnal Sains Komunikasi dan Pengembangan Masyarakat* **2021**, *5*, 509–521, doi:10.29244/jskpm.v5i3.845.

18. Hartoyo, A.P.P.; Pamoengkas, P.; Mudzaky, R.H.; Khairunnisa, S.; Ramadhi, A.; Munawir, A. Estimation of vegetation cover changes using NDVI in Mount Halimun Salak National Park, Indonesia. *IOP Conference Series: Earth and Environmental Science* **2022**, *1109*, 012068, doi:10.1088/1755-1315/1109/1/012068.

19. Rahmawati, R.; Hernawan, D.; Darusman, D.; Sektiono, D. Performance of forest governance implementation Mountain Halimun Salak National Park. *Sosiohumaniora* **2019**, *21*, 305–315, doi:10.24198/sosiohumaniora.v21i3.7328.

20. Sardjo, S.; Dharmawan, A.H.; Darusman, D.; Wahyuni, E. The agricultural expansion in conservation areas: The case of Gunung Halimun Salak National Park, West Java. *Forest and Society* **2022**, *6*, 742–762, doi:10.24259/fs.v6i2.18380.

21. Wulansari, M.; Fawzi, I.L. The role of the kehati foundation in the Halimun Salak green corridor initiative program. *Jurnal Ilmu Kesejahteraan Sosial* **2020**, *21*, 1–13, doi:10.7454/jurnalkessos.v21i1.245.

22. Purwatiningsih, S.D. The understanding of the local community around the forest regarding forest conservation information in utilizing and preserving the forests of Gunung Halimun Salak National Park. *IKRA-ITH Humaniora* **2022**, *6*, 110–120.

23. Hartoyo, A.P.P.; Azis, S.N.; Ramadhi, A.; Khairunnisa, S.; Mudzaky, R.H.; Pamoengkas, P.; Fadillah, A.; Ruliandi, A. Vegetation cover changes and species composition: preliminary results from agroforestry system in Gunung Halimun Salak National Park, Indonesia. *IOP Conference Series: Earth and Environmental Science* **2023**, *1145*, 012011, doi:10.1088/1755-1315/1145/1/012011.

24. Khairunnisa, S.; Pamoengkas, P.; Hartoyo, A.P.P. Analysis of NDVI and plant vegetation diversity in the traditional zone, Mount Halimun Salak National Park, Bogor. *Journal of Natural Resources and Environmental Management* **2024**, *14*, 109–118, doi:10.29244/jpsl.14.1.109.

25. Paul, R.; Patra, S.; Banerjee, K. Socio-economic impact on vulnerability of tropical forests of Eastern Ghats using hybrid modelling. *Tropical Ecology* **2020**, *61*, 475–486, doi:10.1007/s42965-020-00106-5.

*26.* Maryudi, A.; Devkota, R.R.; Schusser, C.; Yufanyi, Y.; Salla, M.; Aurenhammer, H.; Rotchanaphatharawit, R.; Krott, M. Back to basics: considerations in evaluating the outcomes of community forestry. *Forest Policy and Economics* **2012***,* 14, 1–5.

27. Jelas, I.M.; Zulkifley, M.A.; Abdullah, M.; Spraggon, M. Deforestation detection using deep learning-based semantic segmentation techniques: A systematic review. *Frontiers in Forests and Global Change* **2024**, *7*, 1–24, doi:10.3389/ffgc.2024.1300060.

28. Wahab, M.A.A.; Surin, E.S.M.; Nayan, N.M. An approach to mapping deforestation in permanent forest reserve using the convolutional neural network and Sentinel-1 synthetic aperture radar. *International Conference on Information Retrieval and Knowledge Management (CAMP)* **2021**, *vol*, 59–64, doi:10.1109/CAMP51653.2021.9498144.

29. Karaman, K. Deforestation detection in the Amazon with Sentinel-1 SAR image time series. In ISPRS Annals of the Photogrammetry, Remote Sensing and Spatial Information Sciences, ISPRS Geospatial Week 2023, Cairo, Egypt, 2–7, September 2023; pp. 835–842.

30. Ball, J.G.; Petrova, K.; Coomes, D.A.; Flaxman, S. Using deep convolutional neural networks to forecast spatial patterns of Amazonian deforestation. *Methods in Ecology and Evolution* **2022**, *13*, 2622–2634, doi:10.1111/2041-210X.13953.